

Hund's rule-driven Dzyaloshinskii-Moriya interaction at 3d-5d interfaces

A. Belabbes^{1,*}, G. Bihlmayer², F. Bechstedt³, S. Blügel², and A. Manchon^{1†}

¹ King Abdullah University of Science and Technology (KAUST), Physical Science and Engineering Division (PSE)
Thuwal 23955-6900, Saudi Arabia

² Peter Grünberg Institut and Institute for Advanced Simulation, Forschungszentrum Jülich and JARA, D-52425 Jülich
Germany and

³ Institut für Festkörpertheorie und -optik, Friedrich-Schiller-Universität Jena, Max-Wien-Platz 1, 07743 Jena, Germany
(Dated: March 5, 2024)

Using relativistic first-principles calculations, we show that the chemical trend of Dzyaloshinskii–Moriya interaction (DMI) in 3d-5d ultrathin films follows Hund's first rule with a tendency similar to their magnetic moments in either the unsupported 3d monolayers or 3d-5d interfaces. We demonstrate that, besides the spin-orbit coupling (SOC) effect in inversion asymmetric noncollinear magnetic systems, the driving force is the 3d orbital occupation and their spin flip/mixing processes with the spin-orbit active 5d states control directly the sign and magnitude of the DMI. The magnetic chirality changes are discussed in the light of the interplay between SOC, Hund's first rule, and the crystal field splitting of *d* orbitals.

PACS numbers: 75.70.Ak, 71.15.Rf, 71.70.Gm, 75.70.Tj

Introduction Chiral objects are ubiquitous in science [1] and pose fundamental challenges such as the importance of chiral molecules in commercial drugs [2] or the dominance of matter over antimatter in the universe. Magnetic materials lacking inversion symmetry can host chiral magnets and present a unique platform for the exploration and control of chiral objects. The dynamic development of this field has been recently illustrated by the observation of the magnon Hall effect [3, 4] or the achievement of room temperature magnetic skyrmions [5–8], opening avenues for robust high density data storage [9].

A crucial ingredient for the generation of such chiral textures is the Dzyaloshinskii-Moriya antisymmetric magnetic interaction (DMI) [10, 11] arising from spin-orbit coupling (SOC) in inversion asymmetric magnets. Originally proposed in the context of Mott insulators [11], weak metallic ferromagnets and spin glasses [12], major attention has been recently drawn toward the nature of DMI at transition-metal (TM) interfaces. Such interfaces, consisting of a stack of 3d/5d(4d) transition metals, have been intensively investigated from the viewpoint of mainstream spintronics resulting in the recent development of spin-orbit torques [13, 14] and domain wall-based devices [15]. In these systems, the interfacial DMI gives rise to several exotic magnetic phases such as Néel domain walls [16, 17], spin spirals [18], and skyrmions with a defined chirality [5–7, 19].

The ability to understand and control the sign and strength of DMI remains the big challenge of research in magnetism and may open new approaches to future nanoscale magnetic devices [20]. It demands a qualitative description of the physics of DMI that can serve as a guideline for materials and interface design. While such models are available in the context of Mott insulators [11], spin glasses [12] and magnetic Rashba gases [21], such a phenomenology is still lacking for transition-

metal interfaces. In fact, the high complexity of interfacial hybridization hinders the development of qualitative and quantitative predictions in these materials combinations. Only few isolated examples have been investigated from first principles [22–28]. It is therefore crucial to apply such studies and examine the trends of DMI across 3d/5d transition metal interfaces, in order to identify the underlying physical mechanisms and develop a predictive physical picture.

In this Letter, we present the first systematic and comprehensive theoretical analysis of DMI for a large series of 3d transition metals (V, Cr, Mn, Fe, Co, Ni) as overlayers on 5d-TMs (W, Re, Os, Ir, Pt, Au) substrates. We demonstrate that the sign and magnitude of DMI are directly correlated to the degree of 3d-5d orbital hybridization around the Fermi energy, which can be controlled by the intra-atomic Hund's exchange field of the 3d overlayer [29, 30].

First-principles method In order to understand the behavior of DMI in 3d-5d ultrathin films we have performed density functional theory (DFT) calculations in the local density approximation (LDA) [31] to the exchange correlation functional, using the full potential linearized augmented plane wave (FLAPW) method in film geometry [32] as implemented in the Jülich DFT code FLEUR [33]. Both collinear and noncollinear magnetic configurations have been studied employing an asymmetric film consisting of six substrate layers of 5d-TM covered by a pseudomorphic 3d-TM monolayer on one side of the film at the distance optimized for the energetically lowest collinear magnetic state. For the non-collinear calculations we used a $p(1\times 1)$ unit cell applying the generalized Bloch theorem [34]. We considered 512 and 1024 \mathbf{k}_{\parallel} -points in the two-dimensional Brillouin zone (2D-BZ) for calculations including the scalar-relativistic effects and SOC treated within first-order perturbation theory, respectively. More details on the computation

of the spin-spiral and DMI contribution are given in the Supplementary Material [35].

Magnetism of 3d/5d interfaces In Fig. 1(a) we display the variation of the magnetic moment across the 3d/5d interfaces for their magnetic ground state at equilibrium interlayer distances. A major trend appears: Mn overlayer has the highest magnetic moment, regardless of the substrate, and it gradually decreases for chemical elements on both sides of Mn in the 3d TM row of the periodic table. The magnetic moment, although reduced by about 1-3 μ_B , qualitatively follows the total spin S of the 3d shell. This trend reveals that the intra-atomic exchange is controlled by the atomic-like nature of the orbitals according to Hund's first rule [29, 36, 37]. We note that the local magnetic moment of the 3d/5d films (solid lines) is reduced with respect to the magnetic moment of the (ideal) unsupported monoatomic 3d layers (UML - dashed line). This is a consequence of the increased bonding at the interface due to the orbital hybridization of surface and overlayer states [see Fig. 1(a)].

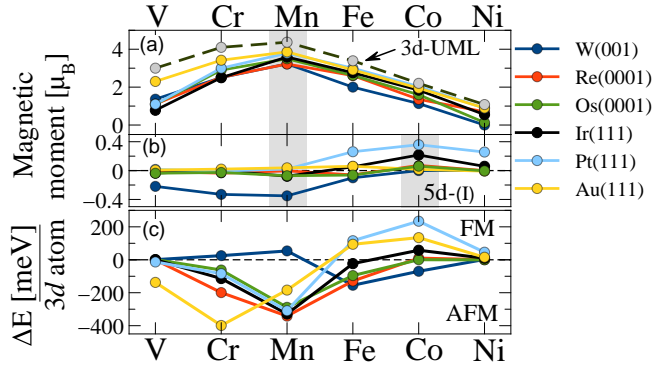


FIG. 1. (Color online) (a) Calculated magnetic moments of the 3d TM monolayers on 5d substrates compared to the moments of 3d UML indicated by the dashed black line. (b) The magnetic moments of interface 5d atoms [38]. (c) The magnetic order of 3d monolayers on 5d substrates using different configurations: FM state, row-wise $p(1 \times 2)$ - and checkerboard $c(2 \times 2)$ -AFM states for the square lattice (001), FM and AFM for the (111) and (0001) oriented surfaces. Positive $\Delta E = E_{\text{AFM}} - E_{\text{FM}}$ indicates a FM ground state, while negative values denote an AFM order.

Fig. 1(b) shows that the substrate exhibits an induced spin polarization since the increased bonding with 3d overlayer enhances the magnetic moment of the neighboring 5d atoms at the interface. From this figure we conclude that W, Pt and to some extent Ir are highly polarizable substrates, while the other substrates considered show a relatively small induced magnetic moment at the interface. The induced magnetic moment for Pt and W substrates couples ferromagnetically and antiferromagnetically with the 3d overlayer, respectively. Their strong local-spin polarizability is mainly due to the high spin susceptibility originating from the large Stoner exchange parameter. For the Au substrate, on the other

hand, there is almost no or only very weak polarization since the 3d orbitals do not hybridize with the energetically low-lying 5d states of Au.

To complete the description of the transition-metal interfaces, we analyze the magnetic stability of 3d overlayers on various 5d substrates in terms of the total energy difference $\Delta E = E_{\text{AFM}} - E_{\text{FM}}$ as shown in Fig. 1(c). We primarily focus on three collinear configurations: the FM state, row-wise $p(1 \times 2)$ -AFM state for (111) and (0001) surfaces and the checkerboard $c(2 \times 2)$ -AFM states for (001) oriented surfaces (see Fig. 1 in the Supplementary Material [35]). For a W(001) substrate, we clearly observe the opposite trend for the early 3d overlayer elements V, Cr, and Mn compared to all other considered 5d substrates, in good agreement with the theoretical study by Ferriani *et al.* [37], who predicted the same energetic ordering for 3d/W(001). We find that the magnetic ground state is AFM for all substrates, while it is FM for W with small energy differences between the two magnetic configurations. In the case of Mn/W(001) the row-wise $p(1 \times 2)$ -AFM state is energetically more favorable than the checkerboard $c(2 \times 2)$ -AFM configuration by ~ 0.3 eV/Mn atom. However, for Ni, Co, and Fe, moving from right to left through the 5d elements, we observe a strong tendency from FM ordering toward an AFM coupling as a function of the 5d band filling of the substrate.

We notice that the 3d-5d interface states around the Fermi energy and their relative lineup control the competition between FM and AFM coupling of the deposited 3d atoms [37, 39, 40]. This especially holds when the nearest-neighbor exchange interaction $\Delta E = E_{\text{AFM}} - E_{\text{FM}}$ is small as shown in Fig. 1(c). In this case, complex magnetic textures can be expected in the presence of SOC since the antisymmetric exchange DM interaction [10, 11] contributes considerably to the total energy. Indeed, if it is sufficiently strong to compete with the magnetocrystalline anisotropy and the Heisenberg exchange, it can stabilize long-range chiral magnetic order such as skyrmions or homochiral spin spirals [18, 19].

Dzyaloshinskii-Moriya interaction Phenomenologically, the DMI has the typical form $E_{\text{DM}} = \sum_{i,j} \mathbf{D}_{ij} \cdot (\mathbf{S}_i \times \mathbf{S}_j)$, where \mathbf{D}_{ij} determines the strength and sign of DMI, and \mathbf{S}_i and \mathbf{S}_j are magnetic spin moments located on neighboring atomic sites i and j (see Supplementary Material for more details [35]). The energy contribution to DMI due to SOC treated in first order perturbation theory corresponds to the sum of all energy shifts from filled states, $E_{\text{DMI}}(\mathbf{q}) = \sum_{k\nu}^{\text{occ.}} n_{k\nu}(\mathbf{q}) \delta \epsilon_{k\nu}(\mathbf{q})$, with $n_{k\nu}(\mathbf{q})$ as the occupation numbers of state $|\psi_{k\nu}(\mathbf{q})\rangle$ (ν -band index, \mathbf{k} -Bloch vector) and \mathbf{q} as the wave-vector propagation of the spin-spiral. Here, the energy shift of the occupied states with respect to the scalar-relativistic (SR) calculation corresponds to $\delta \epsilon_{k\nu} = \epsilon_{k\nu}^{\text{SOC}} - \epsilon_{k\nu}^{\text{SR}}$. In the limit of smooth magnetic textures ($\mathbf{q} \rightarrow 0$), the DMI can be directly determined by a linear fit $E_{\text{DMI}}(\mathbf{q}) \approx Dq$

[41]. In order to further understand the layer-resolved DMI energy $E_{\text{DMI}}^\mu(\mathbf{q})$ (μ labels the atom in the unit cell), we consider the site decomposition of the SOC operator $\mathcal{H}_{\text{so}} = \sum_\mu \xi(r^\mu) \sigma \cdot \mathbf{L}^\mu$, where ξ is the SOC strength related to the spherical muffin-tin potential $V(r^\mu)$, $\xi \sim r^{-1} dV/dr$, $\mathbf{r}^\mu = \mathbf{r} - \mathbf{R}^\mu$ and $|\mathbf{r}^\mu| < R_{\text{MT}}^\mu$. \mathbf{R}^μ references the center and R_{MT}^μ is the radius of the μ th muffin-tin sphere, and μ runs over all atoms in the unit cell.

The central result of this Letter is summarized in Fig. 2(a) (see also Tables I and II in [35]). There the total DMI energy D^{tot} is represented as a function of the 3d overlayer element for various 5d substrates. Apart from 3d/Au(111) interfaces, the calculations reveal a very surprising trend in which the modulus of the D -vector, i.e., the DMI energy divided by the square of the spin magnetic moment $M_{3d/5d}^2$, across the 3d/5d interfaces follows Hund's first rule with a tendency similar to their magnetic trends in either the 3d UML or 3d/5d ultrathin films [see Fig. 2(b)]. In low dimensional systems the spin moments as function of the number of d electrons are well described by Hund's first rule [29, 36, 40, 42]. For the D -vector, such a correlation has been neither experimentally nor theoretically demonstrated for 3d/5d thin films. This fact is surprising as it is opposite to what was expected from the knowledge of magnetism in bulk and thin films, especially in view that such a correlation does not hold for the proximity induced magnetization, Heisenberg exchange parameters, J_{ij} , and the magnetic energy anisotropy [20, 40, 43–45] [see also Fig. 1(a-b-c) and Fig. 2]. Indeed, the nearest-neighbor exchange interaction (J_1) for 3d TMs follows perfectly the Bethe-Slater curve and not Hund's first rule [45]. More specifically, since DMI emerges from a complex interplay between (i) degree of spin-polarization of 3d/5d interface atoms and their band filling, (ii) strength of SOC in the underlying heavy metal 5d-substrate, and (iii) the inversion symmetry breaking at the interface, one does not necessarily expect a direct correlation between the magnetism of the 3d overlayer and the DMI. In the discussion part we will explain in more detail the physical reasons behind the unexpected trend.

In Fig. 2(a) the largest absolute DMI values are obtained for Mn/5d films, regardless of the substrate, with a maximum value of 17 meV nm for Mn/W(001). They monotonically decrease toward V and Ni atoms. In contrast, despite the large SOC of Au, DMI in 3d/Au almost vanishes due to the completely filled d shell of the Au substrate, irrespective of the 3d overlayer [see Fig. 2(a)]. This remarkable finding demonstrates that the DMI does depend critically not only on SOC and lack of the inversion symmetry, but also on the d wavefunction hybridization of the studied 3d/5d interface. The latter affects significantly the interlayer hopping of electrons and, consequently, the magnetic coupling between the 3d overlayer. It is also worthwhile to note that most

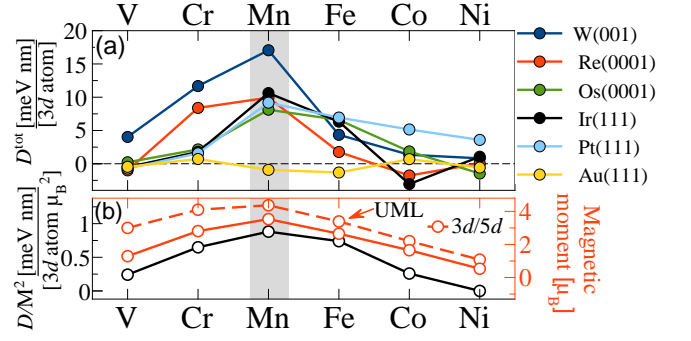


FIG. 2. (Color online) (a) Strength and sign of Dzyaloshinskii–Moriya interaction (DMI) D^{tot} in 3d TM monolayers on 5d substrates calculated around their magnetic ground state combining the relativistic SOC effect with spin spirals. A positive sign of D^{tot} indicates a left-rotational sense or "left chirality". (b) correlation between $E_{\text{DMI}} \sim D^{\text{tot}}/M_{3d/5d}^2$ averaged over 3d/5d interfaces (black line) versus the adlayer, the magnetic moments in 3d TM UML (dashed red line), and the local magnetic moment per atom averaged over 3d/5d interfaces (solid red line).

of 3d/5d interfaces have a positive sign of DMI, left- or right-rotating depending on their magnetic ground state [cf. Fig. 1(c) and Fig. 2].

Discussion For the analysis below, it is worth emphasizing that the delocalized 5d wave functions are responsible for the SOC matrix elements $\mathcal{H}_{\text{so}}(\xi\mathbf{L})$ and make essential contributions to DMI [see Fig. 3(a)]. This behavior is confirmed by the layer-resolved DMI parameter D^μ [Fig. 3(b)], which indicates that the sign and strength of DMI are mainly ascribable to the large contribution of the 5d surface: 80% of the total DMI strength D^{tot} comes from the first two 5d surface layers depending only weakly on the 3d overlayer. An analogous behavior has been identified for the Rashba effect, where 90% of the Rashba splitting is dominated by 5d surface state wavefunction [46, 47]. However, despite the weak SOC in the 3d overlayer their intra-atomic exchange field can easily modify the electronic structure around the Fermi energy and consequently change the strength of DMI.

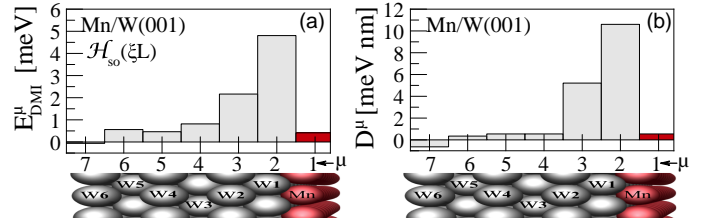


FIG. 3. (Color online) (a) Layer-resolved $E_{\text{DMI}}^\mu(\mathbf{q})$ to the energies of long-period lengths for Mn/W(001) and (b) the DMI-strength D^μ is extracted through a linear fit [$E_{\text{DMI}}^\mu(\mathbf{q}) \approx D^\mu q$]. Note, the positive sign of D^{tot} ($D^{\text{tot}} = \sum_\mu D^\mu$) indicates a left chirality.

The results displayed in Figs. 1 and 2 demonstrate a systematic correlation between DMI and magnetic moment on the one hand, and DMI and the energetic positions of 3d/5d states on the other hand. This mechanism can be understood by examining the band-alignment of the 3d and 5d states and their spin flip/mixing processes, since the anisotropic exchange mechanism requires spin-flip transitions between occupied and unoccupied states that involve spin-orbit active states [11, 22]. Note that the intermediate 5d states are necessary for spin-flip process to unoccupied states of the other spin channel.

The basic idea is illustrated in Fig. 4, where the electronic configuration of 3d orbitals and their spin-split band positions with respect to 5d-W states are displayed. Since the 5d bandwidth is significantly larger than the crystal field splitting and the 5d states are weakly polarized (degenerate and partially filled), the overall physics is mostly governed by the band lineup of 3d spin channels, themselves determined by Hund's first rule. According to this rule, for the V and Ni overlayers both spin channels are almost occupied or unoccupied and consequently transitions between these states do not contribute anymore to the DMI. We emphasize that the occupied and unoccupied states should be available for the 3d electrons to allow for spin-flip excitations. In the case of Co, some spin-down states become unoccupied and transitions into these states contribute only weakly to the DMI. However, in the case of Mn the filling of the five Mn-3d orbitals adopts a stable "high spin state" due to the small crystal-field splitting between the t_{2g} and e_g shells [see Fig. 4]. As a result, the spin-up (spin-down) channels are entirely occupied (unoccupied) and all transitions contribute to DMI through the intermediate spin-orbit active 5d states. In other words, the 3d-5d-3d electron hopping is facilitated, resulting in a large DMI. Note that the situation is almost similar for the half-filled Fe and Cr atoms but the *exchange splitting* is reduced where most of the Fe spin-down (Cr spin-up) states are still unoccupied (occupied). This fact clearly explains the sensitivity of DMI on the choice of 3d overlayer in Fig. 2. Since the electronic configuration of the 5d orbitals is governed by either the bandwidth or crystal field splitting, these scenarios are valid for all 3d/5d interfaces, irrespective of the substrate. The Au substrate is an exception since the spin-orbit 5d states should dominate at the Fermi level and have to be energetically close to unoccupied minority spin states to facilitate the spin-flip processes necessary for the DMI.

Based on the above scenarios, the interplay between Hund's exchange, crystal field splitting, and SOC should be generally considered in any "design" of the DMI. The band-lineup determined by Hund's rule controls not only the 3d spin-flip transitions states but also their spin-mixing processes with the spin-orbit active 5d states [see Fig. 2 and Fig. 4]. Summarizing the results for all 3d/5d interfaces, we conclude that for an interface with 3d overlayer that has a band gap around the Fermi en-

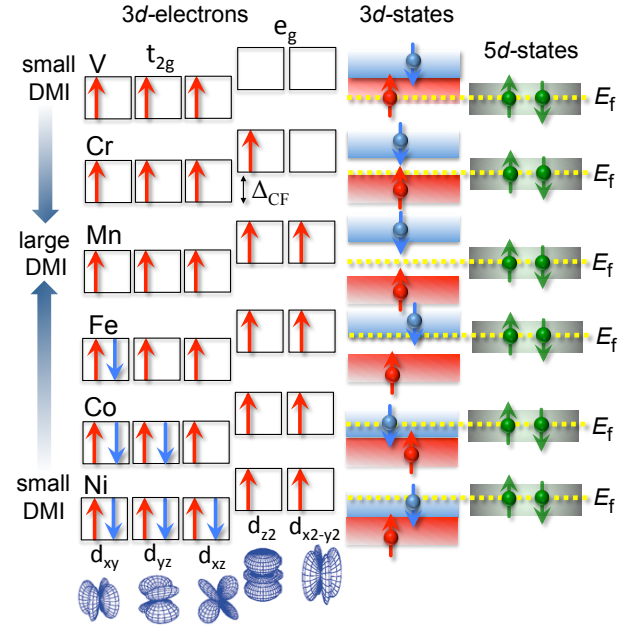


FIG. 4. (Color online) Left side: filling with electrons of 3d TMs elements into the five 3d-orbitals according to Hund's first rule, spin-up and -down are shown by red and blue arrows, respectively. On the right side we show the spin-split band positions of 3d states with respect to 5d-W states. Note, since the 5d bandwidth is significantly larger than the crystal field splitting the 5d states are degenerate at the Fermi level. Δ_{CF} indicates the crystal-field splitting between the t_{2g} and e_g shells.

ergy in both spin channels, a rather large DMI energy should be expected. This fact also relates to the gradual decrease of DMI for chemical elements on both sides of Mn in the 3d TM row of the periodic table, although in low-symmetry environments additional factors may play a role [27]. In this context, atomic Hund's first rule is a powerful guideline to control the sign and magnitude of DMI in particular since the total energy contribution also involves a proportionality to $M_{3d/5d}^2$.

In summary, we have predicted the systematic trend of the DMI in 3d-5d ultrathin films using first-principles calculations. In particular, we demonstrated that the sign and strength of DMI depend strongly on degree of hybridization between 3d-5d states around the Fermi level. Furthermore, in addition to (i) strength of SOC in the underlying heavy metal 5d-substrate, (ii) the degree of the inversion symmetry breaking at the interface and (iii) 5d band filling, we show that the driving force behind the peculiar behavior of DMI is the 3d/5d band-lineup controlled by the Hund's rule filling of 3d shells, which also plays a decisive role in the general picture of spin dynamics. We anticipate that our prediction will provide guidance for the experimental realization and further investigation of chiral properties of ultra-thin magnetic films.

A.B. and A.M. acknowledge financial support from

the King Abdullah University of Science and Technology (KAUST) through the Award No OSR-CRG URF/1/2285-01 from the Office of Sponsored Research

(OSR). We acknowledge computing time on the supercomputers SHAHEEN, NOOR, and SMC at KAUST Supercomputing Centre and JUROPA at the Jülich Supercomputing Centre (JSC).

Supplemental Materials: Hund's rule-driven Dzyaloshinskii-Moriya interaction at 3d-5d interfaces

Spin-spiral and Dzyaloshinskii-Moriya Interaction (DMI)

In order to investigate the DMI, first we self-consistently calculate the total energy of homogeneous magnetic spin-spirals employing the generalized Bloch theorem within the scalar-relativistic approach [34]. We have considered the energy dispersion $E(\mathbf{q})$ of planar spin spirals which are the general solution of the Heisenberg Hamiltonian, i.e., states in which the magnetic moment of an atom site \mathbf{R}_i is given by $\mathbf{M}_i = M[\cos(\mathbf{q} \cdot \mathbf{R}_i), \sin(\mathbf{q} \cdot \mathbf{R}_i), 0]$ where \mathbf{q} is the wave vector propagation of the spin spiral. By imposing the Néel spin spirals along the high-symmetry lines of 2D-BZ in either square or triangular lattices, we can scan all possible magnetic configurations that are described by a single \mathbf{q} vector. So, varying the \mathbf{q} vector with small steps along the paths connecting the high-symmetry points, we find the well-defined magnetic phases, for hexagonal lattices: FM state at $\bar{\Gamma}$ -point ($\mathbf{q}=0$), RW-AFM state at the \bar{M} -point, and periodic 120° Néel state at the \bar{K} -point, while for square lattice, we find FM state at $\bar{\Gamma}$ -point, RW $p(1 \times 2)$ -AFM state at the \bar{X} -point, and \bar{M} -point characterizes the checkerboard $c(2 \times 2)$ -AFM (see Fig. 5). When the energy $E(\mathbf{q})$ along the high-symmetry lines of 2D-BZ is lower than any of the collinear magnetic phases studied previously, the system most likely adopts an incommensurate spin-spiral magnetic ground state structure.

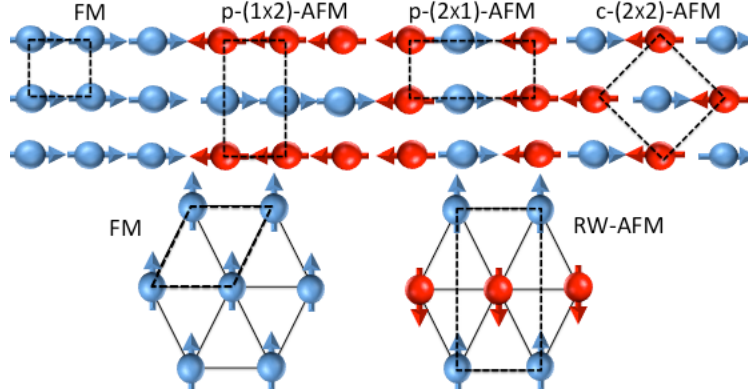


FIG. 5. (Color online) Unit cell sketch of the investigated magnetic configurations of 3d-TMs on 5d substrates: FM state, row-wise $p(1 \times 2)$ - or $p(2 \times 1)$ - and checkerboard $c(2 \times 2)$ -AFM states for the square lattice (001) (upper row), FM and row-wise AFM for the (111) and (0001) oriented surfaces (lower row). For the substrates the ground-state crystal structures bcc (W), hexagonal (Re, Os), and fcc (Ir, Pt, Au) with corresponding surface orientations (001) (W), (0001) (Re, Os), and (111) (Ir, Pt, Au) are investigated.

In a second step, we evaluate the DMI contribution from the energy dispersion of spin-spirals by applying the spin-orbit coupling (SOC) treated within first-order perturbation theory combined with the micromagnetic model [41, 48]. Phenomenologically, the antisymmetric exchange interaction DMI has the typical form $E_{\text{DM}} = \sum_{i,j} \mathbf{D}_{ij} \cdot (\mathbf{S}_i \times \mathbf{S}_j)$, where \mathbf{D}_{ij} is the DM vector which determines the strength and sign of DMI, and \mathbf{S}_i and \mathbf{S}_j are magnetic spin moments located on neighboring atomic sites i and j . Considering the Néel-type out-of-plane configuration the \mathbf{D}_{ij} vector should be oriented in plane and normal to the \mathbf{q} vector Fig. 6(c). Note that the DMI term must vanish for both configurations, Néel-type in-plane and Bloch-type spin spirals, due to symmetry arguments [41] [see Fig. 6(a)(b)]. According to our definition, the vector chirality is characterized by $\mathbf{C} = C\hat{\mathbf{c}} = \mathbf{S}_i \times \mathbf{S}_{i+1}$, where the direction of the vector spin chirality $\hat{\mathbf{c}}$ is considered as spin rotation axis. Thus, left-handed (right-handed) spin spirals correspond to $C = +1$ ($C = -1$).

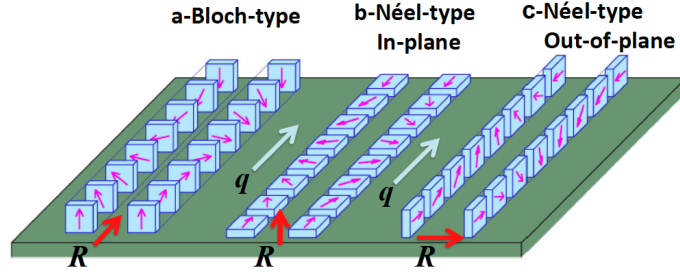


FIG. 6. (Color online) Schematic representation of spin-spirals with different propagation directions \mathbf{q} and spin-rotation axis \mathbf{R} (adapted from [49]). (b,c) Néel-type in-plane and out-of-plane ($\mathbf{R} \perp \mathbf{q}$), respectively and (a) Bloch-type with ($\mathbf{R} \parallel \mathbf{q}$). Note that the DMI vanishes for Néel-in-plane and Bloch-type due to symmetry arguments.

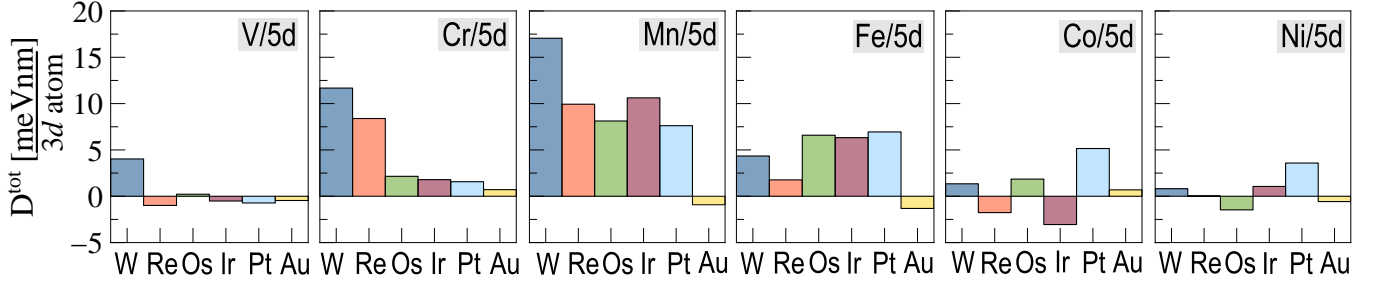


FIG. 7. (Color online) Strength and sign of Dzyaloshinskii–Moriya interaction D^{tot} in 3d TM monolayers on 5d substrates calculated around their magnetic ground state using the combination of the relativistic effect SOC with the spin spirals. A positive sign of D^{tot} indicates a left-rotational sense or "left chirality".

TABLE I. Calculated magnetic moments of the 3d TM monolayers on 5d substrate and interface 5d(I) atoms at their ground state.

TM	$\mu_{\text{mag-3d}} [\mu_B]$						$\mu_{\text{mag-5d(I)}} [\mu_B]$					
	W(001)	Re(0001)	Os(0001)	Ir(111)	Pt(111)	Au(111)	W(001)	Re(0001)	Os(0001)	Ir(111)	Pt(111)	Au(111)
V	1.36	1.09	1.10	0.78	1.10	2.30	-0.22	-0.01	-0.04	-0.03	0.01	0.00
Cr	2.50	2.90	2.52	2.50	3.00	3.42	-0.33	-0.03	-0.03	0.00	0.00	0.02
Mn	3.22	3.49	3.22	3.58	3.79	3.86	-0.35	-0.00	-0.07	-0.08	0.02	0.04
Fe	2.00	2.62	2.61	2.76	3.00	2.91	-0.10	-0.06	-0.06	0.05	0.26	0.06
Co	1.13	1.60	1.36	1.84	2.03	1.94	0.00	0.07	0.06	0.21	0.36	0.02
Ni	0.01	0.13	0.70	0.55	0.89	0.90	0.00	0.00	0.00	0.06	0.25	0.00

TABLE II. Strength and sign of Dzyaloshinskii–Moriya interaction D^{tot} in 3d TM monolayers on 5d substrates calculated around their magnetic ground state using the combination of the relativistic effect SOC with the spin spirals. A positive sign of D^{tot} indicates a left-rotational sense or "left chirality". The total energy differences ΔE , positive $\Delta E = E_{\text{AFM}} - E_{\text{FM}}$ indicates a FM ground state, while negative values denote AFM order.

TM	$D^{\text{tot}} [\text{meV nm}/3d \text{ atom}]$						$\Delta E [\text{meV}/3d \text{ atom}]$					
	W(001)	Re(0001)	Os(0001)	Ir(111)	Pt(111)	Au(111)	W(001)	Re(0001)	Os(0001)	Ir(111)	Pt(111)	Au(111)
V	4.03	-0.99	0.22	-0.51	-0.73	-0.46	0.7	-0.6	0.9	0.1	-13.3	-137.3
Cr	11.68	8.39	2.15	1.78	1.57	0.71	25.1	-199.1	-62.2	-113.7	-84.3	-398.8
Mn	17.06	9.94	8.12	10.62	9.18	-0.92	53.6	-341.7	-288.6	-328.7	-309.1	-184.0
Fe	4.35	1.77	6.59	6.32	6.94	-1.32	-154.6	-128.8	-95.9	-23.2	115.7	94.0
Co	1.35	-1.77	1.85	-3.05	5.15	0.69	-70.0	10.0	0.3	57.8	234.0	134.5
Ni	0.81	0.03	-1.47	1.06	3.58	-0.57	2.0	0.7	-0.1	9.8	45.8	15.3

* abderrezak.belabbes@kaust.edu.sa

† aurelien.manchon@kaust.edu.sa

- [1] D. K. Kondepudi *et al.*, *Sci. Am.* **262**, 108 (1990).
- [2] A. R. Maureen, *Chem. Eng. News* **82**, 47 (2004).
- [3] Y. Onose *et al.*, *Science* **329**, 297 (2010).
- [4] A. Manchon *et al.*, *Phys. Rev. B* **90**, 224403 (2014).
- [5] C. Moreau-Luchaire *et al.*, *Nat. Nano.* **11**, 444 (2016).
- [6] O. Boulle *et al.*, *Nat. Nano.* **11**, 449 (2016).
- [7] W. Jiang *et al.*, *Science* **349**, 283 (2015).
- [8] Y. Tokunaga *et al.*, *Nat. Commun.* **6**, 7638 (2015).
- [9] A. Fert *et al.*, *Nat. Nano.* **8**, 152 (2013).
- [10] I. Dzyaloshinsky, *Sov. Phys. JETP* **4**, 241 (1958).
- [11] T. Moriya, *Phys. Rev.* **120**, 91 (1960).
- [12] A. Fert and P. M. Levy, *Phys. Rev. Lett.* **44**, 1538 (1980).
- [13] I. M. Miron *et al.*, *Nature* **476**, 189 (2011).
- [14] L. Liu *et al.*, *Nat. Phys.* **8**, 561566 (2014).
- [15] S. H. Yang *et al.*, *Nat. Nano.* **10**, 221 (2015).
- [16] A. Thiaville *et al.*, *Europhys. Lett.* **100**, 57002 (2012).
- [17] K. S. Ryu *et al.*, *Nat. Nano.* **8**, 527533 (2013).
- [18] M. Bode *et al.*, *Nature* **447**, 190 (2007).
- [19] S. Heinze *et al.*, *Nature Physics* **7**, 713 (2011).
- [20] A. Belabbes *et al.*, *Sci. Rep.* **6**, 24634 (2016).
- [21] K.-W. Kim *et al.*, *Phys. Rev. Lett.* **111**, 216601 (2013).
- [22] V. Kashid *et al.*, *Phys. Rev. B* **90**, 054412 (2014).
- [23] S. Bornemann *et al.*, *Phys. Rev. B* **86**, 104436 (2012).
- [24] E. Simon *et al.*, *J. Phys. Cond. Matt.* **26**, 186001 (2014).
- [25] B. Dupé *et al.*, *Nat. Commun.* **5**, 4030 (2014).
- [26] B. Zimmermann *et al.*, *Phys. Rev. B* **90**, 115427 (2014).
- [27] B. Schweflinghaus *et al.*, *Phys. Rev. B* **94**, 024403 (2016).
- [28] Y. Hongxin *et al.*, *Phys. Rev. Lett.* **115**, 267210 (2015).
- [29] F. Hund, *Z. Phys.* **40**, 742 (1927).
- [30] A. A. Khajetoorians *et al.*, *Nat. Nano.* **10**, 958 (2015).
- [31] J. P. Perdew *et al.*, *Phys. Rev. B* **23**, 5048 (1981).
- [32] E. Wimmer *et al.*, *Phys. Rev. B* **24**, 864 (1981).
- [33] URL <http://www.flapw.de>.
- [34] P. Kurz *et al.*, *Phys. Rev. B* **69**, 024415 (2004).
- [35] See Supplementary Material for details of the calculation.
- [36] S. Blügel, *Phys. Rev. Lett.* **68**, 851 (1992).
- [37] P. Ferriani *et al.*, *Phys. Rev. B* **72**, 024452 (2005).
- [38] The AFM order does not show any induced spin polarization at the interface layer for symmetry reasons.
- [39] F. Bechstedt, *Principles of Surface Physics* (Springer-Verlag, Berlin, 2003).
- [40] S. Blügel and G. Bihlmayer, *Magnetism of Low-dimensional Systems: Theory*, edited by H. Kronmüller and S. Parkin (Handbook of Magnetism and Advanced Magnetic Materials, 2007) pp. 598–640.
- [41] M. Heide *et al.*, *Phys. Rev. B* **78**, 140403 (2008).
- [42] L. de' Medici *et al.*, *Phys. Rev. Lett.* **107**, 256401 (2011).
- [43] J. Gayles *et al.*, *Phys. Rev. Lett.* **115**, 036602 (2015).
- [44] K.-S. Ryu *et al.*, *Nat. Commun.* **5**, 3910 (2014).
- [45] Y. O. Kvashnin *et al.*, *Phys. Rev. Lett.* **116**, 217202 (2016).
- [46] G. Sergiy *et al.*, *Phys. Rev. B* **93**, 174421 (2016).
- [47] G. Bihlmayer *et al.*, *Surf. Sci.* **600**, 3888 (2006).
- [48] M. Heide *et al.*, *Phys. B: Cond. Matt.* **404**, 2678 (2009).
- [49] M. Heide *et al.*, *Spin Orbit Driven Physics at Surfaces* (Psi-k scientific highlight No. 78, 2006).